







# Human follicular fluid elicits select dose- and age-dependent effects on mouse oocytes and cumulus–oocyte complexes in a heterologous *in vitro* maturation assay

Shweta S. Dipali <sup>1</sup>, Chanakarn Suebthawinkul <sup>1,2</sup>, Joanna E. Burdette <sup>3</sup>, Mary Ellen Pavone <sup>1</sup>, and Francesca E. Duncan <sup>1,\*</sup>

<sup>1</sup>Department of Obstetrics and Gynecology, Feinberg School of Medicine, Northwestern University, Chicago, IL, USA

<sup>2</sup>Department of Obstetrics and Gynecology, Faculty of Medicine, Chulalongkorn University, Bangkok, Thailand

<sup>3</sup>Department of Pharmaceutical Sciences, University of Illinois at Chicago, Chicago, IL, USA

\*Correspondence address. Department of Obstetrics and Gynecology, Feinberg School of Medicine, Northwestern University, 303 E. Superior St., Lurie 10-117, Chicago, IL 60611, USA. Tel: +1-312-503-2172; E-mail: f-duncan@northwestern.edu  <https://orcid.org/0000-0002-3756-9394>

## Abstract

Follicular fluid (FF) is a primary microenvironment of the oocyte within an antral follicle. Although several studies have defined the composition of human FF in normal physiology and determined how it is altered in disease states, the direct impacts of human FF on the oocyte are not well understood. The difficulty of obtaining suitable numbers of human oocytes for research makes addressing such a question challenging. Therefore, we used a heterologous model in which we cultured mouse oocytes in human FF. To determine whether FF has dose-dependent effects on gamete quality, we performed *in vitro* maturation of denuded oocytes from reproductively young mice (6–12 weeks) in 10%, 50%, or 100% FF from participants of mid-reproductive age (32–36 years). FF impacted meiotic competence in a dose-dependent manner, with concentrations >10% inhibiting meiotic progression and resulting in spindle and chromosome alignment defects. We previously demonstrated that human FF acquires a fibro-inflammatory cytokine signature with age. Thus, to determine whether exposure to an aging FF microenvironment contributes to the age-dependent decrease in gamete quality, we matured denuded oocytes and cumulus–oocyte complexes (COCs) in FF from reproductively young (28–30 years) and old (40–42 years) participants. FF decreased meiotic progression of COCs, but not oocytes, from reproductively young and old (9–12 months) mice in an age-dependent manner. Moreover, FF had modest age-dependent impacts on mitochondrial aggregation in denuded oocytes and cumulus layer expansion dynamics in COCs, which may influence fertilization or early embryo development. Overall, these findings demonstrate that acute human FF exposure can impact select markers of mouse oocyte quality in both dose- and age-dependent manners.

**Keywords:** oocyte / cumulus–oocyte complex / follicular fluid / meiosis / spindle / chromosome / mitochondria / cumulus expansion / reproductive aging

## Introduction

Developmental competence of the female gamete is defined by its ability to be fertilized and sustain early embryo development. Oocytes must undergo both nuclear and cytoplasmic maturation to be developmentally competent (Conti and Franciosi, 2018). Nuclear maturation refers to the processes that allow for the resumption of meiosis I and drive meiotic progression to form a euploid gamete (Conti and Franciosi, 2018). Cytoplasmic maturation encompasses remodeling and repositioning of intracellular organelles, as well as the accumulation of necessary maternal mRNA, proteins, and other macromolecules that will support later fertilization and early preimplantation embryo development prior to genome activation (Conti and Franciosi, 2018). However, these processes are not entirely oocyte-intrinsic mechanisms, and the oocyte is dependent on the microenvironment in which it develops. Cumulus granulosa cells surround the oocyte within the antral follicle and provide metabolic and nutritional

support for the oocyte, in addition to regulating meiotic arrest (Robker *et al.*, 2018). Cumulus cells are physically connected to the oocyte via specialized filopodia, called transzonal projections (TZPs), which traverse the zona pellucida to mediate the movement of small molecules and metabolites from cumulus cells to the oocyte, and are essential for oocyte maturation (Clarke, 2022; Doherty *et al.*, 2022). In addition to cumulus cells, follicular fluid (FF) comprises another primary microenvironment of the oocyte within the antral follicle (Babayev and Duncan, 2022).

FF is a plasma derivative that accumulates in antral follicles through thecal capillaries due to an osmotic gradient driven by the synthesis and secretion of large molecules by granulosa cells (Edwards, 1974; Rodgers and Irving-Rodgers, 2010). FF is heterogeneous in composition, containing hormones, growth factors, reactive oxygen species (ROS), and other metabolites that are necessary for oocytes to acquire developmental competence (Hennet and Combelles, 2012; Emori and Drapkin, 2014). As follicle vascularity, intrafollicular oxygen content, and mitochondrial

Received: January 20, 2023. Revised: October 11, 2023. Editorial decision: November 07, 2023.

© The Author(s) 2023. Published by Oxford University Press on behalf of European Society of Human Reproduction and Embryology. All rights reserved. For permissions, please email: [journals.permissions@oup.com](mailto:journals.permissions@oup.com)

activity are important variables in optimal oocyte development, the balance of ROS and antioxidants in FF is critical (Revelli et al., 2009). Severely hypoxic follicles contain gametes with a high incidence of spindle abnormalities, in turn leading to increased rates of embryonic aneuploidy (Van Blerkom et al., 1997). The total antioxidant capacity in FF is significantly higher in follicles containing fertilization-competent eggs and is positively correlated with embryo quality (Oyawoye et al., 2003; Pasqualotto et al., 2004). Moreover, the hormones found in FF impact oocyte maturation directly, through action on the oocyte, as well as indirectly, by driving secretions from somatic cells within the follicle (Hennet and Combelles, 2012). High FF concentrations of follicle stimulating hormone and luteinizing hormone, as well as estradiol promote successful oocyte maturation and are correlated with high rates of fertilization (Revelli et al., 2009; Hennet and Combelles, 2012). Broadly, FF composition is thought to be indicative of oocyte quality and in fact, several factors within FF have been investigated as biomarkers of oocyte competence (Dumesic et al., 2015).

FF composition is altered in conditions associated with reduced gamete quality. For example, obesity is associated with distinct proteomic and metabolomic FF signatures (Ruebel et al., 2019; Song et al., 2020; Schon et al., 2022). Moreover, FF composition changes significantly with advanced reproductive age (Babayev and Duncan, 2022). Over 200 microRNAs (miRNAs) are present in exosomes or are free-floating within FF; aging is associated with dysregulation of miRNA expression and a greater number of exosomes are present in FF from older women (Sang et al., 2013; Battaglia et al., 2020). Additionally, the metabolites present in FF are significantly altered with reproductive age, including decreased glucose and increased lactate levels, suggesting higher glycolytic activity in the antral follicle (Dogan et al., 2020). Reproductive aging is also associated with decreased levels of the amino acid D-aspartic acid in FF, which is involved in hormone biosynthesis, as well as an altered FF lipidomic profile (D'Aniello et al., 2007; Cordeiro et al., 2018). Advanced glycation end products (AGEs) are toxic molecules that form by non-enzymatic modification of proteins, lipids, or nucleic acids by glucose and AGE action results in a proinflammatory state, as well as cellular damage (Piperi et al., 2012). Increased concentrations of AGEs are present in FF with aging (Takeo et al., 2017). Furthermore, ROS levels are higher in FF from older women (Wang et al., 2020). This increase in FF ROS levels may be due in part to reduced antioxidants, such as melatonin, in FF with advanced age (Zhang et al., 2020). Furthermore, the fibro-inflammatory cytokine profile of FF increases with advanced reproductive age (Bouet et al., 2020; Machlin et al., 2021).

Given that FF composes the local microenvironment of the oocyte, the overarching goal of this study was to determine how FF directly impacts oocyte competence. To this end, we developed a heterologous model in which we matured denuded mouse oocytes and cumulus–oocyte complexes (COCs) in human FF. This model system is necessary due to the limited availability of healthy human oocytes for research purposes and the difficulty in obtaining sufficient quantities of mouse FF for experimentation. We matured denuded mouse oocytes in the presence of 10%, 50%, and 100% FF from participants of mid-reproductive age to determine whether FF has dose-dependent effects on oocyte quality. Moreover, because human FF composition changes with advanced reproductive age, we utilized FF from reproductively young or old women to determine whether mouse oocytes are responsive to the altered environment. FF had dose- but not age-dependent effects on denuded oocyte meiotic maturation.

However, FF decreased maturation of oocytes within intact COCs in an age-dependent manner. Moreover, compared to FF from reproductively young participants, FF from reproductively old participants altered mitochondrial aggregation in denuded oocytes as well as cumulus layer expansion in COCs from reproductively old mice.

## Materials and methods

### Animals

Female CD-1 mice (aged 4–5 weeks) or retired breeders were purchased from Envigo (Indianapolis, IN, USA) and used for experiments at 6–12 weeks (reproductively young) or 9–12 months (reproductively old) of age, respectively. Mice were housed in a controlled barrier facility at Northwestern University's Center for Comparative Medicine (Chicago, IL, USA) under constant temperature, humidity, and light (14 h light/10 h dark). Upon arrival at Northwestern University, animals were provided water and Teklad Global irradiated chow (2916) containing minimal phytoestrogens (Envigo, Indianapolis, IN, USA) *ad libitum*. All animal experiments were performed under protocols approved by the Institutional Animal Care and Use Committee (Northwestern University) and in accordance to the National Institutes of Health Guidelines for the Care and Use of Laboratory Animals.

### Oocyte and cumulus–oocyte complex isolation and *in vitro* maturation

To maximize the yield of oocytes and COCs, mice were hyperstimulated via intraperitoneal injection with 5 IU pregnant mare serum gonadotropin (PMSG, ProSpec-Tany TechnoGene, East Brunswick, NJ, USA) and at 44- to 46-h post-PMSG injection, ovaries were harvested. Antral follicles were mechanically punctured using insulin syringes to release COCs into pre-warmed Leibovitz's Medium (L15, Gibco, Grand Island, NY, USA) containing 3 mg/ml polyvinylpyrrolidone (PVP, Sigma-Aldrich, St Louis, MO, USA), 0.5% penicillin-streptomycin (Pen-Strep, Gibco), and 2.5  $\mu$ M milrinone (Sigma-Aldrich) (L15/PVP/PS+mil). To obtain denuded oocytes from COCs, cumulus cells were stripped mechanically. Germinal vesicle (GV)-intact denuded oocytes were matured for 14–16 h to metaphase of meiosis II (MII) in  $\alpha$ MEM GlutaMAX (Gibco) containing 3 mg/ml Bovine Serum Albumin (BSA, Sigma-Aldrich) and 0.5% Pen-Strep without milrinone (MEM+BSA+PS) at 37°C in a humidified atmosphere of 5% CO<sub>2</sub> in air (Kusuhara et al., 2021; Rogers et al., 2021; Suebthawinkul et al., 2022, 2023). Maturation media was supplemented with 10%, 50%, or 100% human FF as specified in the results for each experiment and in figure legends. Following maturation, gametes were transferred to L15/PVP/PS without milrinone and scored for meiotic progression based on morphological criteria. Transmitted light images were taken on an EVOS FL Auto Cell Imaging System (ThermoFisher Scientific, Waltham, MA, USA) using a 10 $\times$  objective.

Intact COCs were collected and matured for 14–16 h in a specific media that induces and supports cumulus layer expansion ( $\alpha$ MEM GlutaMAX (Gibco) containing 5% Fetal Bovine Serum (FBS, Gibco), 20 mM HEPES (Sigma-Aldrich), 0.25 mM Sodium Pyruvate (Sigma-Aldrich), and 10 ng/ml Epidermal Growth Factor (EGF; Sigma-Aldrich) (MEM+FBS+HEPES+SP+EGF)) at 37°C in a humidified atmosphere of 5% CO<sub>2</sub> in air or in the EmbryoScope+ (Vitrolife, Denver, CO, USA) (Hayashi et al., 2017; Verlhac and Terret, 2018; Suebthawinkul et al., 2022, 2023). For COCs matured in a standard incubator, transmitted light images were taken before and after maturation on an EVOS FL Auto Cell Imaging System using a 10 $\times$  objective to evaluate cumulus expansion. For

culture in the EmbryoScope+, MEM+FBS+HEPES+SP+EGF was pre-equilibrated in EmbryoSlide+ culture dishes (Vitrolife) in the EmbryoScope+ for 16–24 h as previously reported (Suebthawinkul et al., 2022, 2023). Following pre-equilibration, COCs were loaded into EmbryoSlide+ culture dishes as per manufacturer's instructions and matured at 37°C in 5% CO<sub>2</sub> (Suebthawinkul et al., 2022). After maturation, cumulus cells were stripped mechanically following a brief incubation in 0.25 mg/ml hyaluronidase (Sigma-Aldrich), to assess meiotic progression prior to downstream immunocytochemistry.

### Human follicular fluid

Human FF was acquired through the Northwestern University Reproductive Tissue Library (NU-RTL). The NU-RTL is an Institutional Review Board-approved centralized repository for de-identified clinical reproductive specimens for research purposes. In addition, the NU-RTL collects and stores basic de-identified demographic and medical health information from participants. Participants who were 18 years or older at the time of the procedure, were English-speaking, had provided signed informed consent for the NU-RTL, and were undergoing oocyte retrieval for a non-cancerous diagnosis were included in this study. Participants who were younger than 18 years old at the time of the procedure were excluded from this study. FF was obtained by aspiration during oocyte retrieval from participants undergoing ART procedures as previously published (Machlin et al., 2021). Participant information for FF samples used in this study, including age, anti-Müllerian hormone (AMH) levels, body mass index, and infertility diagnosis, is described in [Supplementary Table S1](#). FF from a total of 19 participants (8 reproductively young, 8 reproductively old, 3 mid-reproductive age) was utilized for this study. FF from a single participant per age cohort was used in each replicate of an experiment. Three or more replicates were performed for each experiment, so the data shown includes at least three participants per age cohort. FF was thawed on ice for addition to maturation media. FF did not undergo multiple freeze-thaw cycles.

### Wholemout immunocytochemistry and live cell dyes

After IVM, oocytes were fixed in 3.8% paraformaldehyde (PFA, Electron Microscopy Sciences, Hatfield, PA, USA) and 0.1% Triton X-100 (TX-100, Alfa Aesar, Haverhill, MA, USA) in phosphate-buffered saline (PBS, Thermo Scientific) for 1 h at 37°C for detection of pericentrin,  $\alpha$ -tubulin, and phalloidin or in 2% PFA for 20 min at room temperature for detection of kinetochores with anti-centromere antibody. After fixation, oocytes were washed through DPBS (Gibco) containing 3 mg/ml BSA, 0.01% Tween-20 (Acros Organics, Fair Lawn, NJ, USA), and 0.02% sodium azide (Fluka, Charlotte, NC, USA) (BB), and stored in BB at 4°C until processed for immunodetection. Oocytes were permeabilized for 15 min at room temperature in DPBS containing 3 mg/ml BSA, 0.1% TX-100, and 0.02% sodium azide. Oocytes were then washed twice in BB and incubated in dilutions of primary antibodies overnight at 4°C. Oocytes were washed three times in BB and incubated with secondary antibodies for 1 h at room temperature. Oocytes were then washed three times in BB, mounted in 7  $\mu$ l Vectashield containing 4',6-diamidino-2-phenylindole (DAPI, Vector Laboratories, Burlingame, CA, USA), and slides were stored at 4°C until imaging.

F-actin was labeled using phalloidin Alexa Fluor 633 conjugate (1:50, A22284, Invitrogen, Carlsbad, CA, USA). The following primary and conjugated antibodies were used for immunofluorescence: pericentrin (1:100, 611814, BD Biosciences, San Jose, CA,

USA), anti-centromere antibody (1:200, 15-234, Antibodies Incorporated, Davis, CA, USA), and  $\alpha$ -tubulin Alexa Fluor 488 conjugate (1:100, 5063S, Cell Signaling Technology, Danvers, MA, USA). The following secondary antibodies were used for immunofluorescence: goat anti-mouse Alexa Fluor 568 (1:100, A-11004, Thermo Scientific) and goat anti-human Alexa Fluor 488 (1:100, A-11013, Thermo Scientific).

For mitochondria and mitochondrial superoxide staining, oocytes were incubated in MEM+BSA containing 250 nM MitoTracker Red CMXRos (M7512, Invitrogen) and 2 drops/ml NucBlue (Hoechst 33342, R37605, Invitrogen) or 5  $\mu$ M MitoSox Green (M36006, Invitrogen) and 8.1  $\mu$ M Hoechst 33342 (H3570, Invitrogen), respectively, for 30 min following IVM at 37°C in a humidified atmosphere of 5% CO<sub>2</sub> in air. Following staining, oocytes were washed three times in L15/PVP/PS, transferred to 5  $\mu$ l drops of L15/PVP/PS on a glass bottom dish, and covered in mineral oil. Stained oocytes were imaged immediately on a Leica SP5 inverted laser scanning confocal microscope as described below (Leica Microsystems, Buffalo Grove, IL, USA).

### Confocal microscopy and image analysis

Oocytes were imaged on a Leica SP5 inverted laser scanning confocal microscope (Leica Microsystems) using near-UV (405 nm), argon (488 nm), and two different helium–neon (543 and 633 nm) lasers. For spindle morphology and chromosome alignment analysis, as well as mitochondria and mitochondrial superoxide evaluation, images were captured under a 40 $\times$  oil-immersion objective with the zoom adjusted to fit each oocyte within the field of view. Images were acquired as z-stacks with optical sections taken every 1  $\mu$ m to span the region of the chromosomes. Settings were determined by the Glow-Over Look Up Table (LUT) to ensure that there was no pixel oversaturation. Images were processed using LAS AF (Leica Microsystems) and FIJI software (National Institutes of Health, Bethesda, MD, USA).

Spindle length and pole width were determined using FIJI software. Spindle length was measured by drawing a straight line from pole to pole using pericentrin staining for reference. Spindles that were on an angle were excluded from analysis. Similarly, spindle pole width was measured by drawing a straight line to span the width of the pericentrin staining. In cases where pericentrin staining was punctate,  $\alpha$ -tubulin staining was used as a reference to determine pole width.

Mitochondrial distribution, integrated density, aggregate area, and mitochondrial superoxide integrated density were determined from a single z-slice at the region of the egg containing the metaphase II chromosomes. The integrated density is the product of the area and mean pixel intensity. Mitochondrial distribution was categorized as per previously published parameters (Wang et al., 2009; Zeng et al., 2018). Aggregate area was measured using FIJI software following previously published methods (Yu et al., 2010). Briefly, thresholds were adjusted for each image to allow for simultaneous coverage and distinction of mitochondria. The Analyze Particles function was then used to count the number and area of aggregates. Minimum particle size was set to 0.2  $\mu$ m<sup>2</sup> because the diameter of one individual mitochondrion is 0.5–1  $\mu$ m, thus the area for one mitochondrion is 0.2–0.8  $\mu$ m<sup>2</sup>.

### In situ chromosome counting

Chromosome counts were performed as previously described (Duncan et al., 2009; Chiang et al., 2010). Briefly, after meiotic maturation, Metaphase II-arrested eggs were transferred to MEM+BSA+PS containing 100  $\mu$ M monastrol to collapse the bipolar spindle (Tocris Bioscience, Bristol, UK) for 3 h at 37°C. Following monastrol treatment, eggs were fixed in 2% PFA and

stained with anti-centromere antibody to mark kinetochores. Eggs were imaged on a Leica SP5 inverted laser scanning confocal microscope using near-UV (405 nm) and argon (488 nm) lasers under a 100× oil-immersion objective. Images were acquired as z-stacks with 0.4 μm step size to span the region of the chromosomes. Images were processed using LAS AF and FIJI software. To count chromosomes, each kinetochore was marked in the optical section it first appeared using the ROI Manager in FIJI software and a z-projection of all optical sections was used as a reference. Chromosomes were counted independently by two individuals, one of whom was blinded. A euploid mouse egg has 40 kinetochores. Eggs with greater or less than 40 kinetochores were considered aneuploid.

### ATP measurement

ATP was quantified using CellTiter-Glo 3D Cell Viability Assay (Promega, Madison, WI, USA) as per the manufacturer's instructions. Briefly, samples (20 eggs per well) and ATP standards (10 μM, 1 μM, 100 nM, and 10 nM; Sigma-Aldrich) in a total volume of 100 μl of L15/PVP/PS were added to an opaque-walled 96-well plate. Then 100 μl of CellTiter-Glo 3D Reagent was added to each well and the plate was incubated for 5 min on an orbital shaker, followed by 25 min on a benchtop. Luminescence was read using a Cytation3 plate reader (BioTek, Winooski, VT, USA). ATP concentration was calculated from luminescence by creating a line of best fit using luminescence values from ATP standards and data were reported as averages of two technical replicates (2 wells) per experimental group.

### Cumulus expansion analysis

Cumulus expansion area was measured in transmitted light images using FIJI software by tracing COCs pre- and post-expansion using the freehand line tool and delta expansion area was graphed. Cumulus expansion velocity was determined by measuring the thickness of the cumulus layer every hour of culture in time-lapse images from the EmbryoScope+ following previously published methods (Suebthawinkul et al., 2022). To this end, straight lines were drawn to span the width of the cumulus layer on the side of the COC farthest from the edge of EmbryoSlide+ culture well using EmbryoViewer software. Expansion velocity was calculated using the following formula:

$$\text{Expansion velocity } (\mu\text{m/h}) = \frac{\text{Distance at timepoint 2} - \text{Distance at timepoint 1}}{\text{Time at point 2} - \text{Time at point 1}}$$

Expansion velocity was averaged for every 4 h to determine the average expansion velocity per quartile.

### Statistical analysis

Statistical analysis was performed using GraphPad Prism Software (La Jolla, CA, USA) or R (RStudio, version 4.3.0). T-tests, one-way ANOVAs, or two-way ANOVAs (mixed-effects analysis) followed by Tukey's multiple comparisons tests, chi-square, or Fisher's tests were performed to evaluate differences between experimental groups as indicated in figure legends. *P*-values <0.05 were considered significant. All experiments were performed at least three times and all total oocyte or COC numbers used are specified in figure legends.

## Results

### Experimental paradigm

Although oocytes *in vivo* are exposed to 100% FF within antral follicles, studies that utilize FF to improve developmental outcomes

for oocytes from agricultural species routinely supplement maturation media with only 5–60% FF (Kim et al., 1996; Dell'Aquila et al., 1997; Somfai et al., 2012; Pawlak et al., 2018; Tian et al., 2019). Thus, we first sought to determine whether human FF impacts mouse oocyte competence in a dose-dependent manner. To this end, we matured denuded oocytes from reproductively young mice (6–12 weeks) in media without FF as a control or in media containing 10%, 50%, or 100% human FF from participants in their mid-30s (mid: 32–36 years) to examine dose-dependent effects of FF, independent of age (Fig. 1). We examined the dose-dependent effects of FF supplementation on meiotic progression, spindle morphology, and chromosome alignment (Fig. 1). Once we determined the concentration of FF that had minimal negative impacts on meiotic progression, we matured denuded oocytes from reproductively young mice in media without FF as a control or containing FF from reproductively young (young: 28–31 years) or reproductively old (old: 39–42 years) participants at this concentration to examine age-dependent effects of FF on meiotic progression, spindle morphology, chromosome alignment, ploidy, as well as mitochondrial distribution and function (Fig. 1). To determine whether age-associated perturbations intrinsic to the oocyte could compound the effects of FF from reproductively old participants, we matured denuded oocytes from reproductively young and reproductively old (9–12 months) mice in media without FF or media supplemented with FF from reproductively young or old participants in parallel (Fig. 1). We examined compounded effects of oocytes from reproductively old mice and FF from reproductively old participants on meiotic progression, spindle morphology, and chromosome alignment. Finally, given that oocytes are surrounded by companion cumulus cells, which are in direct contact with FF within antral follicles, we examined whether cumulus cells mediate age-dependent effects of FF on oocytes by maturing intact COCs from reproductively young and old mice in media without FF or media containing FF from reproductively young or old participants (Fig. 1). We assessed cumulus layer expansion, as well as meiotic progression, spindle morphology, and chromosome alignment (Fig. 1).

### Follicular fluid has dose-dependent effects on oocyte meiotic maturation

To determine whether human FF impacts mouse oocyte competence in a dose-dependent manner, we matured denuded mouse oocytes in media without FF as a control or in media containing 10%, 50%, or 100% human FF from participants in their mid-30s to minimize any age-dependent effects. When the meiotic stage of oocytes was scored based on morphological criteria using transmitted light images following IVM, we observed that FF decreased meiotic progression in a dose-dependent manner (Fig. 2A and B). Whereas an average of 94.6 ± 2.7% of gametes from the control group extruded first polar bodies, maturation was significantly reduced with FF treatment, with only 76.7 ± 4.3%, 65.6 ± 8.0%, and 36.8 ± 21.3% of gametes extruding polar bodies in the groups supplemented with 10%, 50%, and 100% FF respectively (*P* < 0.0001; Fig. 2B). In addition to oocytes with an intact GV, oocytes that had undergone GV breakdown (Met I), and eggs that had extruded polar bodies (PBE), we also observed a small number of abnormal gametes that underwent symmetric cleavage during the first meiotic division, and this phenotype was only observed in groups treated with FF (Fig. 2A and B).

To further investigate how FF supplementation affects spindle morphology and chromosome alignment in cells that had undergone PBE, we performed immunocytochemistry using antibodies against α-tubulin to visualize spindle fibers and pericentrin to mark spindle poles (Fig. 2C). The percentage of eggs within each

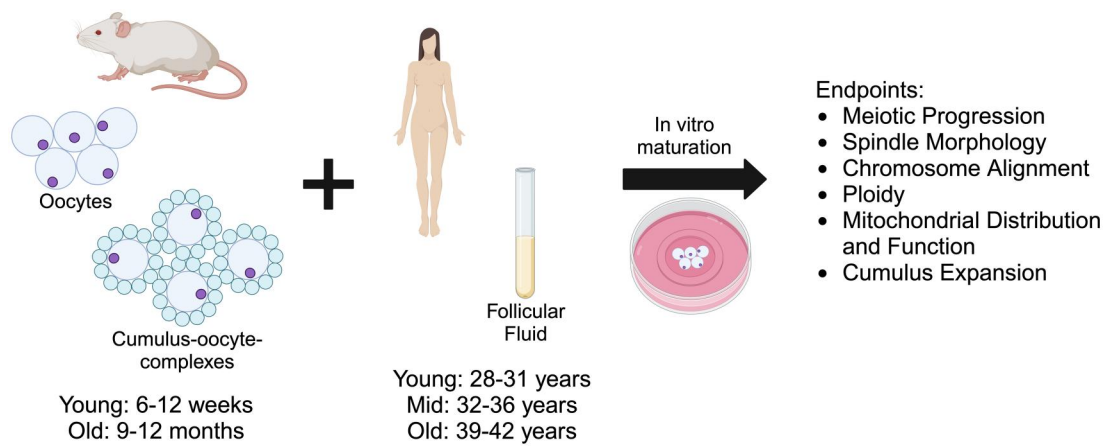


**Figure 1. Schematic of experimental paradigm.** Oocytes and cumulus–oocyte complexes (COCs) from reproductively young (6–12 weeks) and old (9–12 months) mice were matured *in vitro* (IVM) in media supplemented with human follicular fluid (FF) from mid-reproductive age participants (32–36 years) to investigate dose-dependent effects, or with FF from reproductively young (28–31 years) or old (39–42 years) to investigate age-dependent effects, on oocyte quality. Meiotic progression, spindle morphology, chromosome alignment, ploidy, mitochondrial distribution and function, as well as cumulus expansion were evaluated following IVM. This figure was created with BioRender.com.

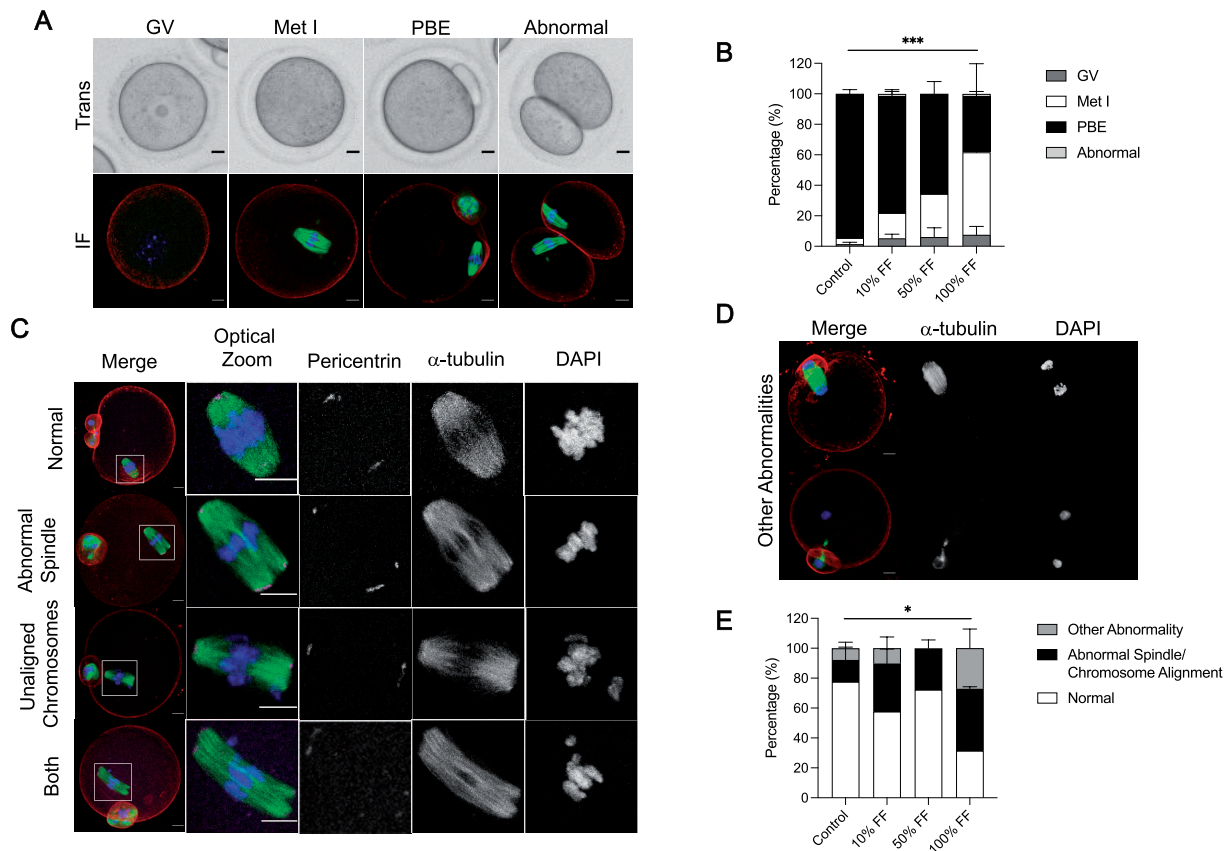


**Figure 2. Follicular fluid (FF) has dose-dependent effects on oocyte meiotic maturation.** (A) Representative transmitted light images (top) and immunofluorescence z-projections (bottom) of each meiotic stage. Oocytes with an intact germinal vesicle (GV), metaphase I (Met I) oocytes, eggs that extruded polar bodies (PBE), and oocytes that underwent symmetric cleavage (abnormal) were identified by morphological criteria. Actin (rhodamine phalloidin, red),  $\alpha$ -tubulin (green), and DNA (DAPI, blue) were detected by immunocytochemistry. Scale bars = 10  $\mu$ m for all panels. (B) Graphs of meiotic progression for oocytes matured in different concentrations of FF. Data are shown as mean  $\pm$  SEM for all panels.  $\chi^2$  (3, N = 235) = 30.84, \*\*\* $P$  < 0.0001 for PBE versus no PBE. N = 56–62 oocytes per group across total of three replicates. (C and D) Representative z-projections of abnormal phenotypes of metaphase II eggs matured in different concentrations of FF. Actin (rhodamine phalloidin, red), pericentrin (magenta),  $\alpha$ -tubulin (green), and DNA (DAPI, blue) were detected by immunocytochemistry. (E) Quantification of abnormal phenotypes in eggs following maturation in different concentrations of FF. N = 13–43 eggs per group across total of three replicates.  $\chi^2$  (3, N = 114) = 9.051, \* $P$  = 0.0286 for normal versus abnormal.

group that had abnormal spindles, unaligned chromosomes, or both phenotypes were assessed (Fig. 2C). We also evaluated oocytes that exhibited cell cycle delays, including anaphase I and

telophase I configurations (Fig. 2D). Overall, an average of 22.4  $\pm$  11.8% of eggs in the control group exhibited one of the aforementioned abnormalities compared to 42.3  $\pm$  4.3%, 27.8  $\pm$  9.8%, and

68.6±23.8% in the groups treated with 10%, 50%, and 100% FF, respectively ( $P=0.0286$ ; Fig. 2E). Thus, FF treatment perturbs meiotic progression and causes an increase of abnormal phenotypes at the highest concentration.

Meiotic spindle size is an indicator of gamete quality (Tomari et al., 2018). In fact, human eggs with spindles between 90 and 120  $\mu\text{m}^2$  in length have higher rates of fertilization, blastocyst formation, and subsequent clinical pregnancy compared to eggs with spindles outside this range (Tomari et al., 2018). Moreover, spindle size is perturbed by treatment with endocrine disrupting chemicals, such as bisphenols, and is altered during post-ovulatory aging, which are both conditions associated with decreased oocyte competence (Kang et al., 2011; Yang et al., 2020). To determine whether FF exposure impacts spindle length and width, we only analyzed eggs that had normal spindle morphology and chromosomes aligned at the metaphase plate following maturation in media supplemented with FF. Treatment with 100% FF resulted in metaphase II spindles that were longer with broader poles relative to untreated controls (Fig. 3A–C). Spindle length (pole-to-pole distance) was an average of  $24.46 \pm 0.63 \mu\text{m}$  in eggs matured without FF compared to  $32.12 \pm 1.36 \mu\text{m}$  in eggs following maturation in 100% FF ( $P=0.0032$ ; Fig. 3A and B). Average pole width was  $4.36 \pm 0.32 \mu\text{m}$  in the control group compared to  $8 \pm 1.61 \mu\text{m}$  in eggs treated with 100% FF ( $P=0.0078$ ; Fig. 3A and C). The average pole width to spindle length ratio was not significantly different between the control and 100% FF groups, indicating that spindles may not be morphometrically different between groups at an individual level (Fig. 3D). However, there was a tendency for an increase in this ratio (Fig. 3D). Given that concentrations higher than 10% FF appear to have a negative impact on meiotic maturation, subsequent studies used 10% FF to investigate the age-dependent effects of FF on oocyte competence.

### Follicular fluid does not impact oocyte meiotic maturation in an age-dependent manner

Advanced reproductive age is associated with reduced oocyte quality and FF composition changes with age (Krisher, 2018; Babayev and Duncan, 2022; Bebbere et al., 2022). To determine whether the aging FF microenvironment may directly contribute to the age-dependent decline in oocyte competence, we matured denuded oocytes in media supplemented with 10% FF from reproductively young ( $30.41 \pm 0.46$  years) and reproductively

old ( $41.57 \pm 0.61$  years) cohorts of participants (Supplementary Fig. S1). Media without FF served as a control. These cohorts were different with regards to age ( $P < 0.0001$ ) and serum AMH levels (young:  $2.79 \pm 0.25 \text{ ng/ml}$ , old:  $1.24 \pm 0.32 \text{ ng/ml}$ ;  $P=0.002$ ), but not body mass index (young:  $22.67 \pm 0.64 \text{ kg/m}^2$ , old:  $21.35 \pm 0.67 \text{ kg/m}^2$ ; Supplementary Fig. S1), suggesting that any impact on gamete competence is more likely to be driven by age relative to BMI. This distinction is important given that supplementation of maturation media with lipid-rich FF collected from obese women has been demonstrated to negatively impact mouse COC maturation and quality (Yang et al., 2012). FF from a single participant per age cohort was used for each experimental replicate, and three or more replicates were performed per experiment. Thus, the data shown includes results of exposure to FF from at least three participants per age cohort. We employed this model of FF exposure from individual participants because if FF samples are pooled, FF from a particular participant(s) may drive results. If robust age effects exist, they should transcend individual participants and be observed consistently across FF samples.

Meiotic progression was not significantly different between groups, and we did not observe any age-dependent effects of FF on spindle morphology, chromosome alignment, or other abnormalities (Fig. 4A and B). Similarly, FF did not have an age-associated impact on the length or width of the metaphase II spindle (Fig. 4C–F).

Aneuploidy is one of the most well-established reproductive age-associated phenotypes (Hassold and Hunt, 2001; Mikwar et al., 2020). To investigate whether FF impacts ploidy in an age-dependent manner, we performed *in situ* chromosome counting in metaphase II eggs after IVM in media supplemented with FF from young or old participants. We did not observe any age-dependent effects of FF on the incidence of aneuploidy, with a similar percentage of eggs matured without FF exhibiting aneuploidy to those matured in media supplemented with FF from young or old participants (Fig. 4G and H). When this aneuploidy rate was further stratified by type of aneuploidy, no significant differences were observed between experimental groups (Fig. 4G and I). Nondisjunction, indicating failure of separation of homologous chromosomes, was characterized by gain or loss of one or more chromosome pair, while premature separation of sister chromatids (PSSC), was characterized by gain or loss of individual chromatids. These results suggest that human FF does not affect meiotic maturation of denuded mouse oocytes in an age-dependent manner.

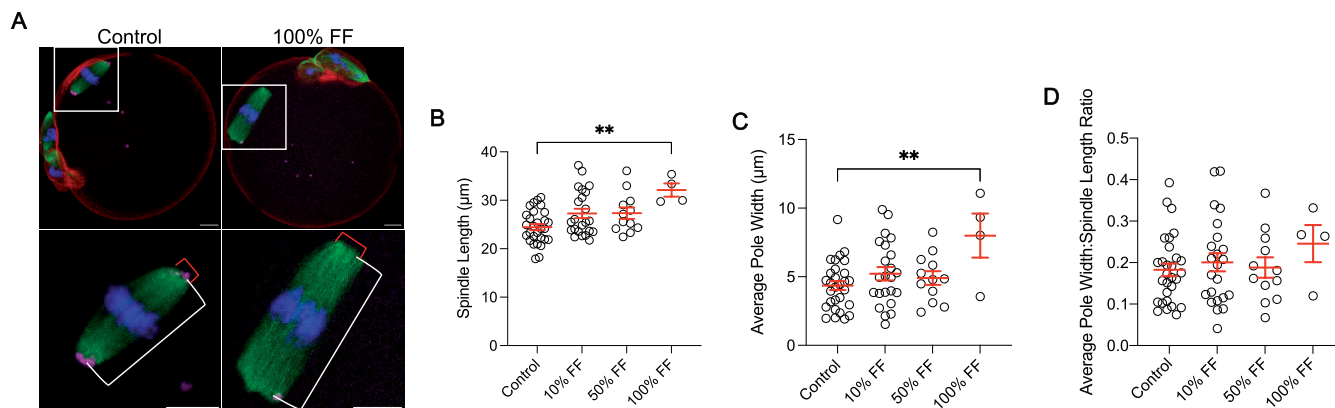


**Figure 3. Follicular fluid (FF) has dose-dependent effects on oocyte spindle morphology.** (A) Representative z-projections of metaphase II spindle length (white bracket) and spindle pole width (red bracket) for eggs following maturation without FF (control) or in 100% FF. Actin (rhodamine phalloidin, red), pericentrin (magenta),  $\alpha$ -tubulin (green), and DNA (DAPI, blue) were detected by immunocytochemistry. Scale bars = 10  $\mu\text{m}$ . (B–D) Quantification of spindle length (B), average pole width (C), and average pole width: spindle length ratio (D) for eggs following maturation in different concentrations of FF. Data are shown as mean  $\pm$  SEM. \*\* $P$ -value  $\leq 0.01$  by one-way ANOVA with multiple comparisons.  $N = 4$ –29 eggs per group across total of three replicates.

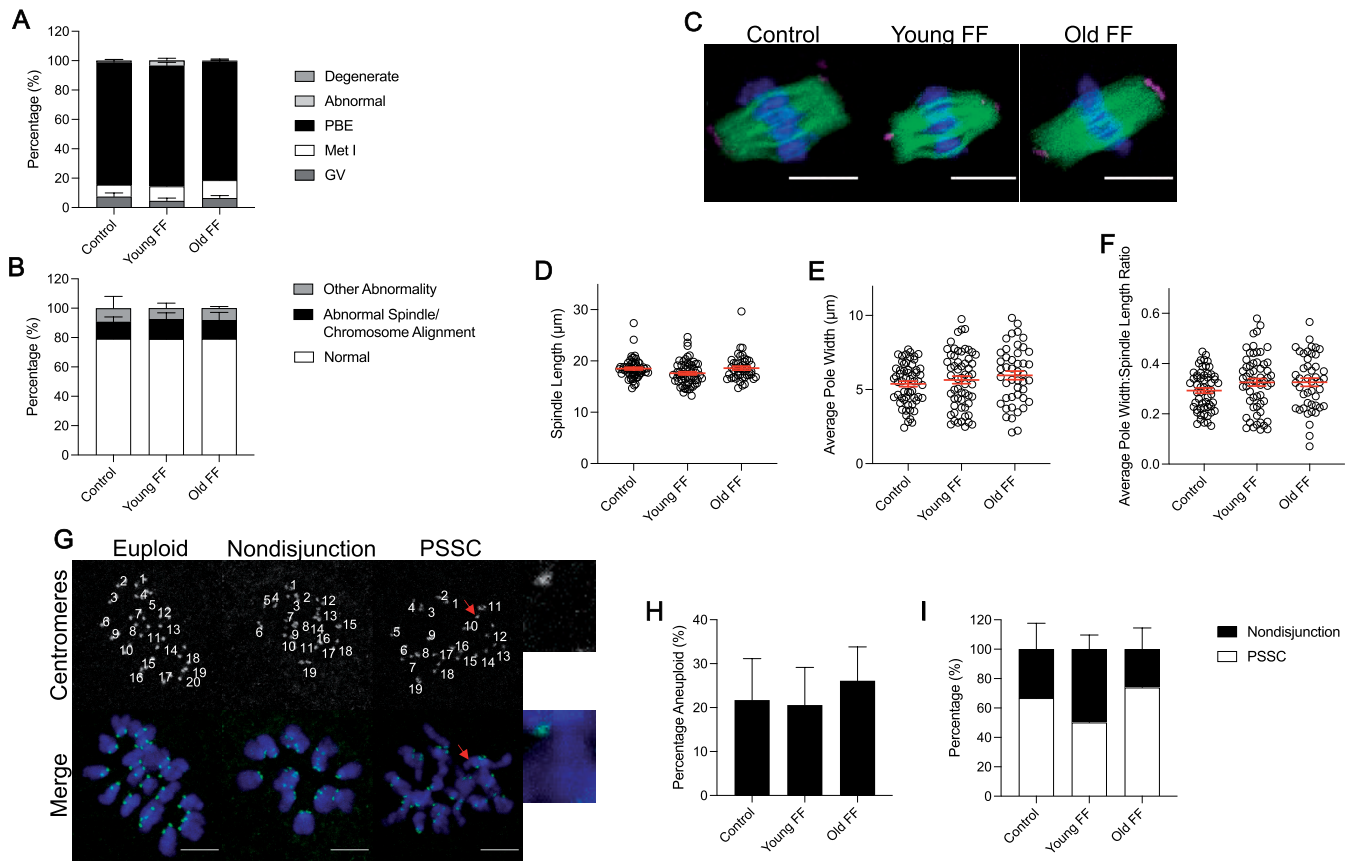


**Figure 4. Follicular fluid (FF) does not impact oocyte meiotic maturation in an age-dependent manner.** (A) Graph of meiotic progression for oocytes matured without FF (control), in young FF, or in old FF. Data are shown as the mean $\pm$ SEM for all panels. N = 234–241 oocytes per group across total of four replicates. (B) Quantification of abnormal phenotypes of metaphase II eggs following maturation without FF (control), in young FF, or in old FF. N = 60–80 eggs per group across total of four replicates. (C) Representative z-projections of metaphase II spindles from eggs following maturation without FF (control), in young FF, or in old FF. Pericentrin (magenta),  $\alpha$ -tubulin (green), and DNA (DAPI, blue) were detected by immunocytochemistry. Scale bars = 10  $\mu$ m. (D–F) Quantification of metaphase II spindle length (D), average pole width (E), and average pole width: spindle length ratio (F) for eggs following maturation without FF (control), in young FF, or in old FF. N = 45–58 eggs per group across total of four replicates. (G) Representative z-projections of metaphase II chromosome spreads from eggs following maturation without FF (control), in young FF, or in old FF. Kinetochores (anti-centromere antibody, green) and DNA (DAPI, blue) were detected by immunocytochemistry. Images labeled with number of kinetochore pairs (top, white). Unpaired kinetochores/chromatids indicated by arrows (red). Scale bars = 5  $\mu$ m. (H–I) Quantification of aneuploidy rates for eggs following maturation without FF (control), in young FF, or in old FF (H) further divided into nondisjunction or premature separation of sister chromatid (PSSC) errors (I). N = 54–63 eggs per group across total of three replicates.

### Oocytes from reproductively young and old mice respond similarly to follicular fluid exposure

All the experiments performed thus far utilized oocytes isolated from reproductively young mice. However, it is possible that age-associated perturbations intrinsic to the oocyte could compound the effects of FF from reproductively old participants, resulting in more pronounced phenotypes. To determine whether oocytes from reproductively old mice may be more susceptible to maturation defects due to FF exposure, we matured denuded oocytes from reproductively young and old mice in FF from both reproductively young and old participants in parallel. Surprisingly, supplementation with FF from reproductively young participants, but not from old participants, significantly decreased meiotic progression compared to untreated controls in oocytes from young mice ( $P=0.005$ ), but not old counterparts (Fig. 5A). As with eggs from reproductively young mice, FF supplementation did not have an age-dependent impact on chromosome alignment in eggs from reproductively old mice (Fig. 5Bi and ii). However, without any FF treatment, gametes from reproductively old mice exhibited a significant increase in chromosome alignment errors ( $24.4 \pm 2.9\%$ ) compared to young counterparts ( $9.3 \pm 2.6\%$ ), as has been previously demonstrated ( $P=0.0179$ ; Fig. 5Biii) (Liu and

Keefe, 2008; Cheng et al., 2017). FF exposure significantly reduced spindle length in eggs from reproductively old mice, regardless of the participant age (control:  $21.47 \pm 0.45 \mu$ m; young FF:  $18.92 \pm 0.43 \mu$ m; old FF:  $19.01 \pm 0.4 \mu$ m;  $P=0.002$ ; Fig. 5C and D). FF did not affect average spindle pole width or average pole width to spindle length ratio in an age-dependent manner in eggs from reproductively young or old mice (Fig. 5Ei, ii and Fi, ii). However, average spindle pole width was increased in eggs from reproductively old mice ( $5.9 \pm 0.24 \mu$ m) compared to young counterparts ( $4.6 \pm 0.23 \mu$ m) without FF treatment ( $P=0.0006$ ; Fig. 5Eiii and G). Correspondingly, the average pole width to spindle length ratio was also increased in eggs from old mice in comparison to eggs from young mice ( $P=0.0023$ ; Fig. 5Fiii and G). Overall, these data suggest that denuded oocytes from old mice are not more sensitive to perturbation by FF exposure even when the FF is from an older individual.

### Follicular fluid increases size of mitochondrial aggregates in an age-dependent manner

As a large amount of ATP is required for transcription and translation, mitochondria are essential for oocyte cytoplasmic maturation (Yamada and Isaji, 2011; Babayev and Seli, 2015).

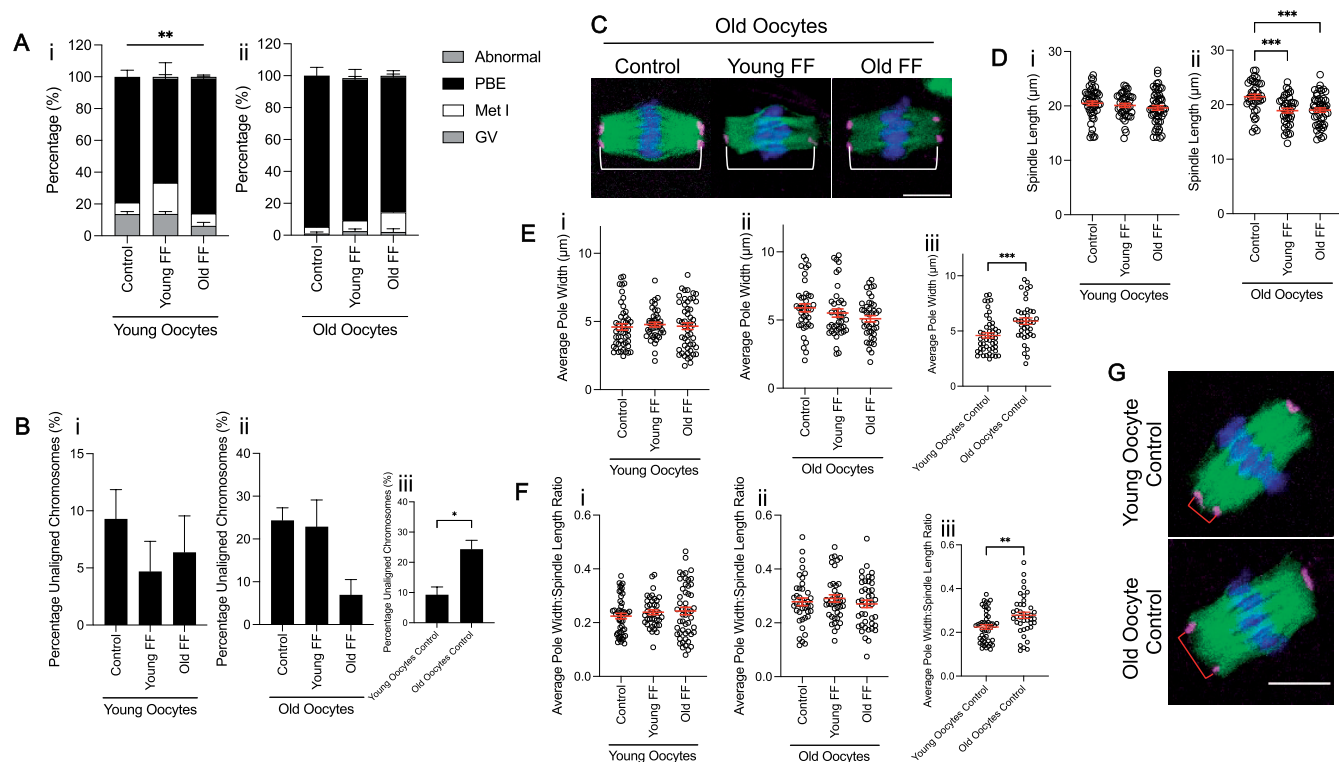


**Figure 5. Oocytes from reproductively young and old mice respond similarly to follicular fluid (FF) exposure.** (A) Graph of meiotic progression for oocytes from young (i) and old (ii) mice matured without FF (control), in young FF, or in old FF. Data are shown as mean $\pm$ SEM for all panels.  $\chi^2$  (2,  $N=231$ )=10.58,  $**P=0.0051$  for young oocytes that extruded polar bodies (PBE) versus no PBE.  $N=60$ –69 oocytes per group across total of three replicates. (B) Quantification of percentage unaligned chromosomes for eggs from young (i) and old (ii) mice following maturation without FF (control), in young FF, or in old FF.  $N=46$ –64 eggs per group across total of three replicates. Inset (iii) compares percentage unaligned chromosomes only for eggs from young and old mice matured without FF.  $*P$ -value  $<0.05$  by t-test. (C) Representative z-projections of metaphase II spindles from eggs from old mice following maturation without FF (control), in young FF, or in old FF. Pericentrin (magenta),  $\alpha$ -tubulin (green), and DNA (DAPI, blue) were detected by immunocytochemistry. Spindle length is indicated by a white bracket. Scale bar = 10  $\mu$ m. (D–F) Quantification of spindle length (D), average pole width (E), and average pole width: spindle length ratio (F) for eggs from young (i) and old (ii) mice following maturation without FF (control), in young FF, or in old FF.  $N=40$ –52 eggs per group across total of three replicates. Insets (iii) compare average pole width (E) and average pole width: spindle length ratio (F) only for eggs from young and old mice matured without FF.  $***P$ -value  $\leq 0.001$ , and  $**P$ -value  $\leq 0.01$  by one-way ANOVA with multiple comparisons (D) or t-tests (E and F). (G) Representative z-projections of metaphase II spindles from eggs from young and old mice matured without FF (control). Spindle pole width is indicated by a red bracket. Immunocytochemistry and scale bar as in (C).

Mitochondria are associated with the spindle following nuclear envelope breakdown until the first meiotic division occurs, are retained in the cytoplasm during PBE, and then are distributed homogeneously through the cytoplasm at the metaphase II arrest (Dalton and Carroll, 2013; Babayev and Seli, 2015). This reorganization of mitochondria is important for spindle organization and distribution of chromosomes during meiosis (Wakai et al., 2014; Kasapoğlu and Seli, 2020). To investigate the age-dependent impact of FF on mitochondrial dynamics, mitochondria in metaphase II eggs were labeled using a live cell dye following IVM in media supplemented with FF from reproductively young or old participants. Mitochondrial distribution was classified as polarized if enriched around the spindle, homogenous if localization was uniform throughout the cytoplasm, or clustering if large aggregates were present, as per previously published criteria (Fig. 6A) (Wang et al., 2009; Zeng et al., 2018). The distribution of mitochondria was not significantly affected by FF treatment (Fig. 6B). However, although not significant, there was a greater tendency for oocytes matured in media containing FF from reproductively old participants to display a clustering mitochondrial distribution than oocytes matured in media without FF or containing FF from reproductively young participants (Fig. 6B). Integrated density was measured to examine age-associated effects of FF on the total amount of mitochondria. Integrated

density was not significantly different between oocytes matured with FF from reproductively young or reproductively old participants compared to those matured without FF (Fig. 6C and D). As the diameter of one individual mitochondrion is 0.5–1  $\mu$ m, and thus the area for one mitochondrion is 0.2–0.8  $\mu$ m<sup>2</sup>, quantification of the proportion of particles larger than 0.8  $\mu$ m<sup>2</sup> allows for analysis of mitochondrial aggregation due to FF treatment. FF treatment did not increase the relative abundance of mitochondrial aggregates as measured by the percentage of particles larger than 0.8  $\mu$ m<sup>2</sup> (Fig. 6C and E). However, FF increased the size of mitochondrial aggregates in an age-dependent manner, with an average aggregate area of 2.46 $\pm$ 0.2  $\mu$ m<sup>2</sup> in eggs treated with FF from reproductively young participants compared to 3.46 $\pm$ 0.32  $\mu$ m<sup>2</sup> in eggs treated with FF from reproductively old participants ( $P=0.0173$ ; Fig. 6C and F). These results demonstrate that FF has age-associated effects on mitochondrial aggregation, but not on the distribution or abundance.

To understand whether there was any functional significance of the larger mitochondrial aggregates in eggs following maturation in FF from reproductively old participants, we assessed ATP concentration and mitochondrial superoxide production. Surprisingly, ATP concentrations were not significantly different in eggs following maturation in FF from either reproductively young or old participants compared to controls matured without



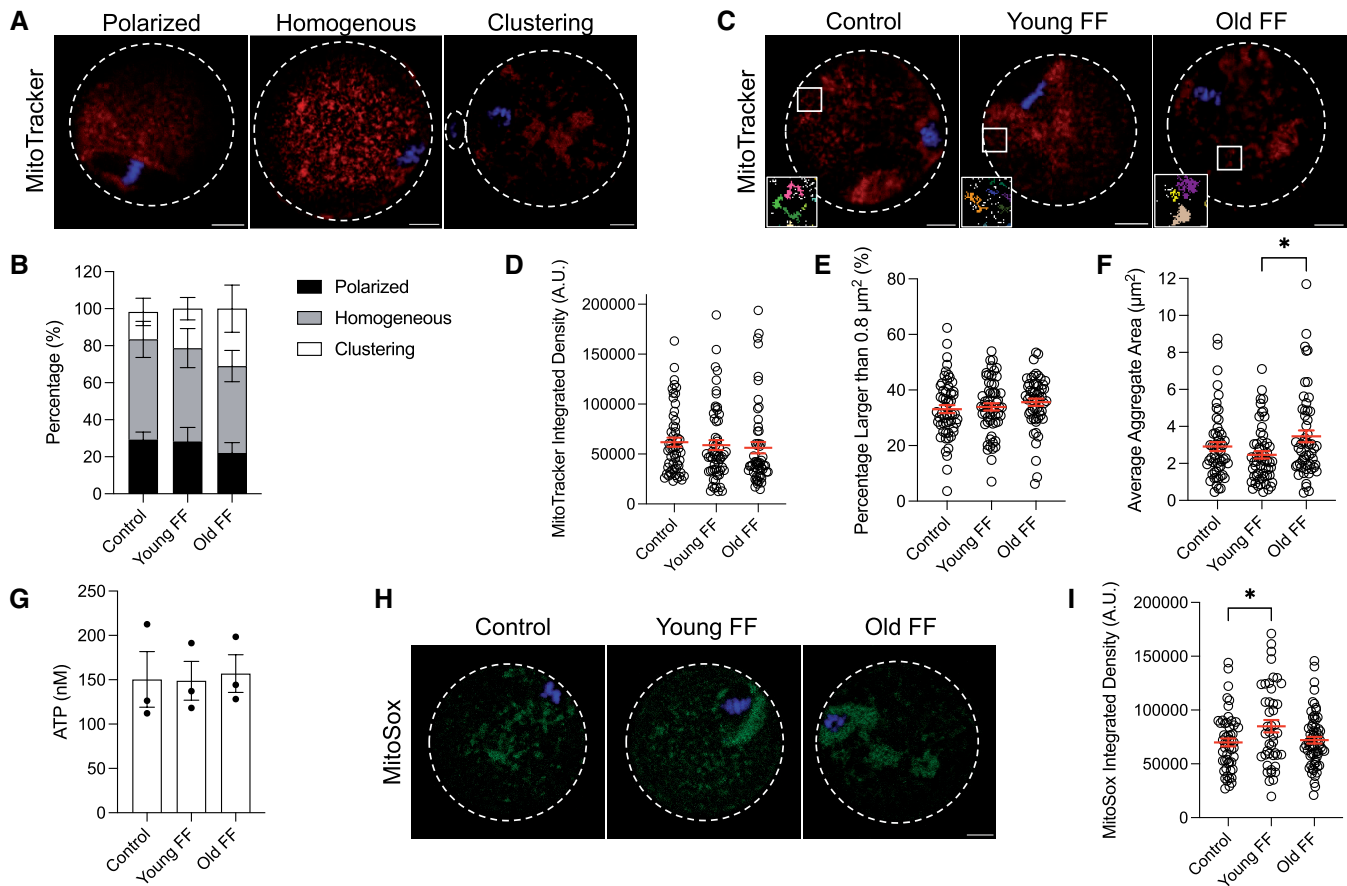


**Figure 6. Follicular fluid (FF) increases size of mitochondrial aggregates in an age-dependent manner.** (A) Representative middle z-slices of different mitochondrial distributions in metaphase II mouse eggs. Mitochondria (MitoTracker, red) and DNA (Hoechst, blue) were visualized by live cell dyes. Dashed lines outline the perimeter of eggs and polar bodies if visible in z-slice. Scale bars = 10  $\mu\text{m}$  for all panels. (B) Quantification of mitochondrial distribution for eggs following maturation without FF (control), in young FF, or in old FF. Data are shown as mean  $\pm$  SEM for all panels. N = 54–58 eggs per group across total of three trials. (C) Representative middle z-slice of eggs following maturation without FF (control), in young FF, or in old FF. Mitochondria and DNA visualized as in (A). Boxed regions are magnified in insets. Insets show representative mitochondrial aggregates following thresholding as quantified in (F). Each color corresponds to one aggregate and particles below the minimum size for quantification are displayed in white. Scale bar (gray) = 1  $\mu\text{m}$ . (D–F) Quantification of mitochondrial integrated density in arbitrary units (A.U.; D), percentage of mitochondrial aggregates larger than 0.8  $\mu\text{m}^2$  (E), and average mitochondrial aggregate area (F). \*P-value  $\leq 0.05$  by one-way ANOVA with multiple comparisons. N = 54–58 eggs per group across total of three trials. (G) Quantification of ATP concentration in eggs following maturation without FF (control), in young FF, or in old FF. Each data point represents the average of two wells (each containing 20 eggs) from one experiment. N = 120 eggs per group across total of three trials. (H) Representative middle z-slice of eggs following maturation without FF (control), in young FF, or in old FF. Mitochondrial superoxide (MitoSox, green) and DNA (Hoechst, blue) were visualized by live cell dyes. (I) Quantification of mitochondrial superoxide integrated density in arbitrary units (A.U.). \*P-value  $\leq 0.05$  by one-way ANOVA with multiple comparisons. N = 44–64 eggs per group across total of four trials.

FF (Fig. 6G). Moreover, mitochondrial superoxide production was higher in eggs matured in FF from reproductively young participants ( $84\,972 \pm 5698$  A.U.) compared to eggs matured without FF ( $69\,873 \pm 3656$  A.U.;  $P = 0.0348$ ) but was not significantly different in eggs matured in FF from reproductively old participants ( $72\,033 \pm 3119$  A.U.; Fig. 6H and I). Taken together, these results suggest that increased mitochondrial aggregate area in eggs following maturation in FF from reproductively old participants does not have an immediate impact on ATP or mitochondrial ROS production.

### Exposure of intact COCs to follicular fluid has age-dependent effects on meiotic progression, but not spindle morphology

Denuded oocytes were used for all experiments described thus far, but oocytes are surrounded by cumulus cells *in vivo*, together forming COCs. Cumulus cells are critical in supporting oocyte development and they are in direct contact with FF within antral follicles. Therefore, it is possible that cumulus cells are

responsive to age-dependent alterations in FF composition, and in turn, mediate the reproductive age-associated decline in oocyte quality. To this end, we matured intact COCs from reproductively young and old mice in media supplemented with FF from reproductively young or old participants, before removing the cumulus cell layer to assess oocyte nuclear maturation parameters. Interestingly, polar body extrusion was significantly decreased in COCs from reproductively young mice matured with FF from reproductively old participants ( $78.8 \pm 18.1\%$ ) compared to COCs matured with FF from reproductively young participants ( $96.4 \pm 3.6\%$ ) or without FF ( $98.4 \pm 1.6\%$ ;  $P = 0.0015$ ; Fig. 7Ai). FF also decreased meiotic progression of COCs from reproductively old mice in an age-dependent manner, similar to what was seen in COCs from young counterparts (control:  $100 \pm 0\%$ ; young FF:  $91.87 \pm 5.1\%$ ; old FF:  $82.44 \pm 6.4\%$ ;  $P = 0.0259$ ; Fig. 7Aii). However, FF did not have an age-effect on chromosome alignment, spindle or other abnormalities, or on morphology of the metaphase II spindle in COCs from reproductively young or old mice (Fig. 7B–E).

## Follicular fluid modestly impacts cumulus expansion dynamics in an age-dependent manner

Cumulus cells produce a hyaluronan matrix in response to the LH surge resulting in expansion of the cumulus layer which is important for ovulation and fertilization (Clarke, 2017; Nagyova, 2018). To determine whether FF has an age-dependent effect on cumulus expansion, we captured transmitted light images of individual COCs from reproductively young and old mice before and after maturation in media supplemented with FF from reproductively young or old participants to assess expansion area (Fig. 8A). The change in total COC area, indicative of cumulus cell layer expansion, was not significantly different due to FF exposure in COCs from reproductively young or old mice (Fig. 8A and B; Supplementary Fig. S2A). However, without any FF treatment, COC expansion area was decreased in COCs from reproductively old mice ( $31\,470.5 \pm 1874.5 \mu\text{m}^2$ ) compared to COCs from reproductively young mice ( $36\,828.373 \pm 1403.7 \mu\text{m}^2$ ) ( $P=0.0215$ ; Fig. 8A and B).

The cumulus cell layer undergoes a characteristic pattern of expansion when monitored in a closed time-lapse imaging system, whereby velocity increases and peaks during the first 8 h of maturation and then decreases (Suebthawinkul et al., 2022, 2023). To specifically investigate whether FF has an age-associated impact on cumulus expansion kinetics, rather than overall expansion area, we analyzed expansion using time-lapse imaging (Fig. 8C; Supplementary Fig. S2B). Cumulus layer thickness was measured for each COC every hour to calculate expansion velocity. Average expansion velocity over the duration of

maturation was unchanged by FF treatment for both COCs from reproductively young and old mice (Supplementary Fig. S2C). However, when further broken down by quartile, age-dependent effects of FF on expansion kinetics were observed (Fig. 8D–F). Specifically, supplementation with FF from both reproductively young ( $3.46 \pm 0.23 \mu\text{m}/\text{h}$ ;  $P=0.0244$ ) and old participants ( $3.76 \pm 0.28 \mu\text{m}/\text{h}$ ;  $P=0.0011$ ) significantly increased average expansion velocity of COCs from reproductively young mice at 12 h compared to untreated controls ( $2.64 \pm 0.15 \mu\text{m}/\text{h}$ ; Fig. 8C and E). Supplementation with FF from reproductively old participants ( $4.16 \pm 0.44 \mu\text{m}/\text{h}$ ) significantly increased average expansion velocity of COCs from reproductively old mice at 12 h compared to untreated controls ( $2.77 \pm 0.23 \mu\text{m}/\text{h}$ ;  $P=0.006$ ; Fig. 8C and F). Although not statistically significant, when cumulus expansion kinetics of COCs from reproductively young and old mice without FF supplementation were interrogated, we observed a trend of decreased expansion velocity at 8 h in old COCs ( $5.17 \pm 0.54 \mu\text{m}/\text{h}$ ) compared to young COCs ( $6.45 \pm 0.32 \mu\text{m}/\text{h}$ ), as has been previously reported (Fig. 8C and D) (Suebthawinkul et al., 2023). Thus, FF exposure has age-associated effects on cumulus expansion kinetics, but not overall cumulus expansion area or velocity.

## Discussion

In this study, we interrogated how human FF may impact oocyte quality using a heterologous IVM assay. We demonstrated that human FF influences mouse oocyte meiotic maturation, including spindle formation in a dose-dependent manner. However, human FF does not have age-dependent effects on meiotic

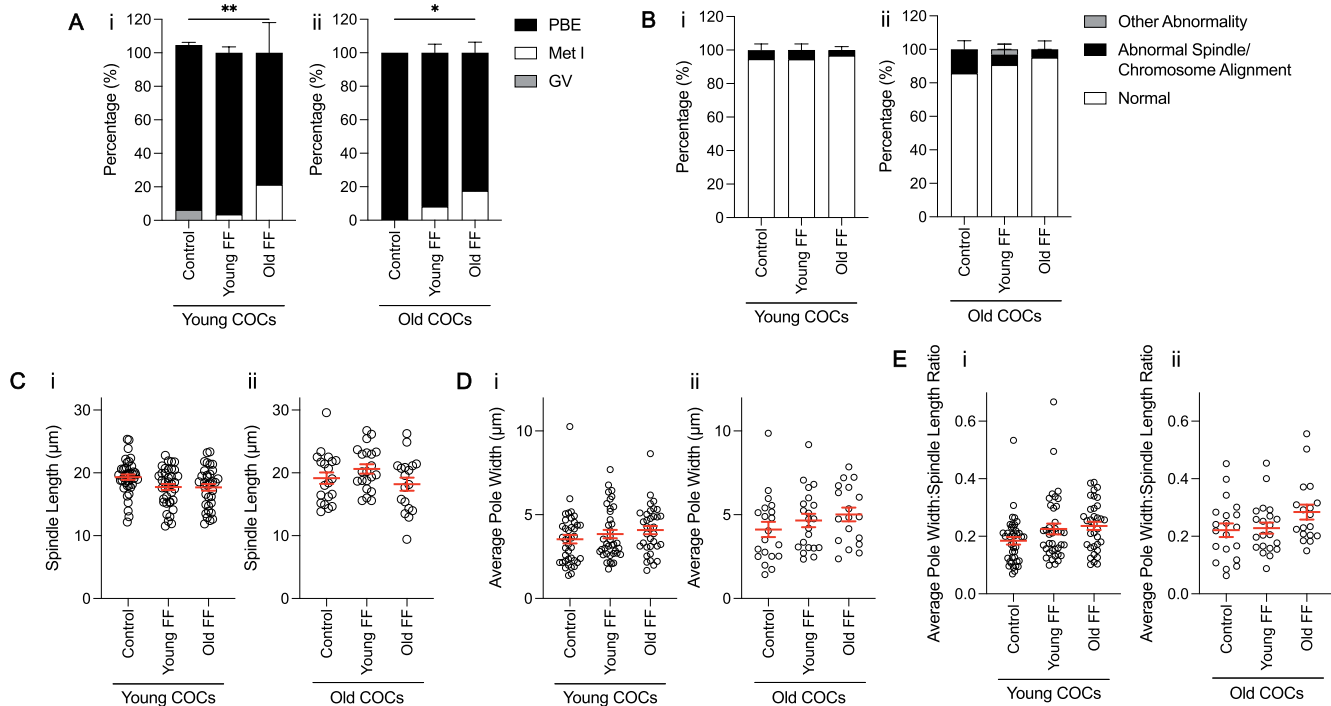


**Figure 7. Exposure of intact cumulus-oocyte complexes (COCs) to follicular fluid (FF) has age-dependent effects on meiotic progression, but not spindle morphology.** (A) Graph of meiotic progression for COCs from young (i) and old (ii) mice matured without FF (control), in young FF, or in old FF. Data are shown as mean±SEM for all panels.  $N=29-56$  COCs per group across total of four trials. (i)  $**P=0.0015$  for young COCs that extruded polar bodies (PBE) versus no PBE by Fisher's exact test. (ii)  $*P=0.0259$  for old COCs PBE versus no PBE by Fisher's exact test. (B) Quantification of abnormal phenotypes of metaphase II eggs from COCs from young (i) and old (ii) mice following maturation without FF (control), in young FF, or in old FF.  $N=24-55$  COCs per group across total of four trials. (C–E) Quantification of spindle length (C), average pole width (D), and average pole width: spindle length ratio (E) for COCs from young (i) and old (ii) mice matured without FF (control), in young FF, or in old FF.  $N=18-40$  COCs per group across total of four trials.

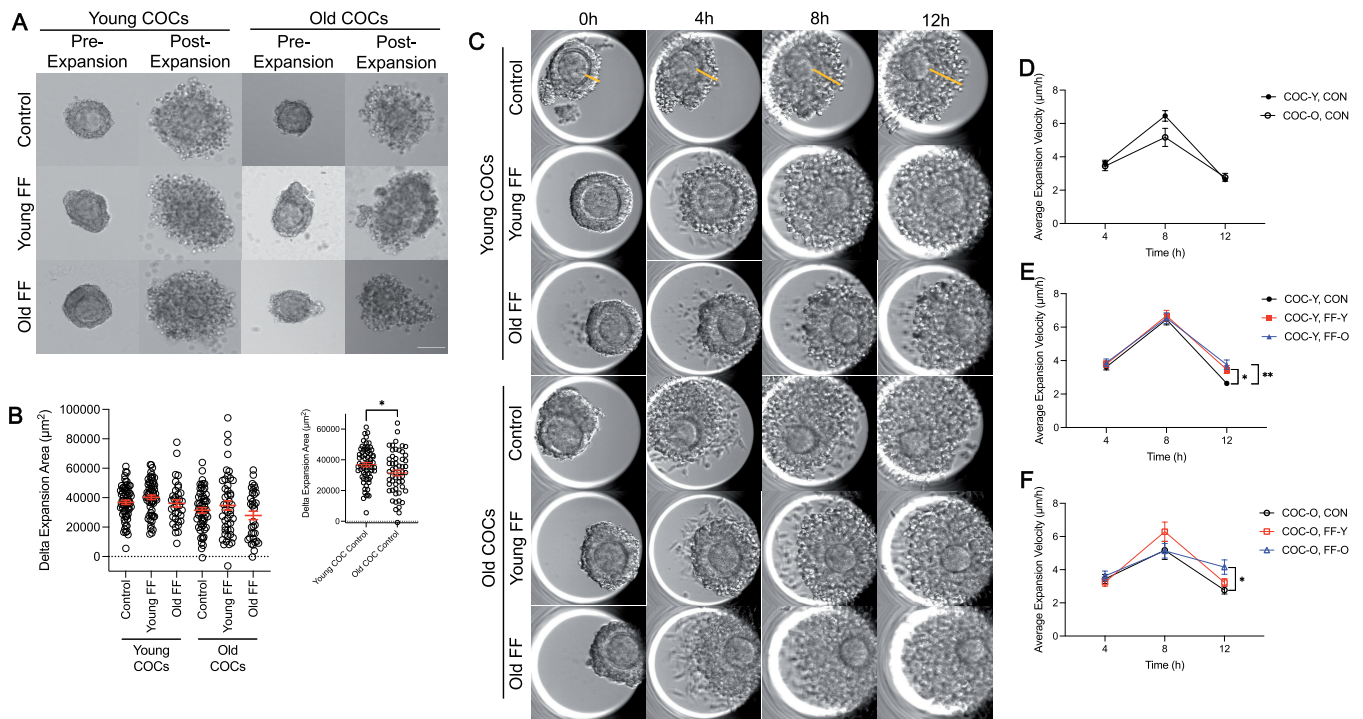


**Figure 8. Follicular fluid (FF) modestly impacts cumulus expansion dynamics in an age-dependent manner.** (A) Representative transmitted light images of COCs from young and old mice pre- and post-expansion without FF (control), in young FF, or in old FF. Scale bar = 10 µm. (B) Quantification of delta (Δ) expansion area for COCs from young and old mice matured without FF (control), in young FF, or in old FF. Data are shown as mean ± SEM for all panels. N = 35–66 COCs per group across total of four replicates. Inset compares delta expansion area only for COCs from young and old mice matured without FF. \*P-value <0.05 by t-test. (C) Representative time-lapse, transmitted light images of COCs from young and old mice matured without FF (control), in young FF, or in old FF. Lines (yellow) indicate cumulus expansion measurements taken to calculate expansion velocity. (D) Quantification of expansion velocity per quartile for COCs from young mice (COC-Y, CON; closed circles) and old mice (COC-O, CON; open circles) matured without FF. (E and F) Quantification of expansion velocity per quartile for COCs from young mice (E, closed shapes) or old mice (F, open shapes) matured without FF (control, CON; black circles), in young FF (FF-Y; red squares), or in old FF (FF-O; blue triangles). N = 54–60 COCs per group across total of four replicates. \*P-value <0.05 and \*\*P-value ≤0.01 by two-way ANOVAs with multiple comparisons.

progression, spindle structure, chromosome alignment, or ploidy of denuded mouse oocytes. Denuded oocytes from reproductively old mice responded similarly to FF exposure as those from young mice. However, human FF had age-dependent effects on mitochondrial aggregate size in denuded oocytes, meiotic progression of intact COCs, as well as on cumulus expansion dynamics in COCs from reproductively old mice. Taken together, these data demonstrate that the FF microenvironment can impact select markers of oocyte competence in both dose- and age-dependent manners.

Although developing oocytes are surrounded by 100% FF within antral follicles, a range of FF concentrations have been utilized to supplement oocyte maturation media in previous studies with agricultural species (Kim et al., 1996; Dell'Aquila et al., 1997; Somfai et al., 2012; Takeo et al., 2017; Pawlak et al., 2018; Tian et al., 2019; Azari-Dolatabad et al., 2021; Park et al., 2021). Most studies do not directly compare the effects of different concentrations of FF, but rather utilize a single concentration to investigate the impacts of FF from different sources or compare the effects of FF supplementation relative to media controls (Dell'Aquila et al., 1997; Somfai et al., 2012; Takeo et al., 2017; Pawlak et al., 2018; Park et al., 2021). Maturation of bovine oocytes in media supplemented with 5% bovine FF enhances re-distribution of active mitochondria and improves COC expansion and fertilization compared to controls (Somfai et al., 2012). Similarly, equine oocytes matured in media containing 20% equine FF displayed increased normal fertilization and developmental potential following intracytoplasmic sperm injection (Dell'Aquila et al., 1997).

The concentrations of FF included in studies that compare multiple doses also vary significantly. For example, a study that examined the effects of supplementation with 1%, 5%, and 10% bovine FF showed that 5% and 10% FF improved bovine blastocyst quality parameters compared to 1% FF and a media-only control (Azari-Dolatabad et al., 2021). Moreover, a study that supplemented mouse oocyte maturation media with 10%, 25%, 50%, or 70% human FF demonstrated that FF specimens collected from follicles containing mature eggs that subsequently underwent fertilization and cleavage, termed mature FF, significantly improved meiotic maturation of mouse oocytes at 50% and 70% concentrations but not at lower doses (Das et al., 1992). This result is contrary to our findings of perturbed mouse oocyte meiotic progression upon supplementation with 50% or 100% human FF. However, we examined rates of PBE after 14–16 h of maturation, whereas this previous study examined PBE after 24 h, meaning that this study may have captured more gametes exhibiting delayed PBE, which we would not have documented (Das et al., 1992). In addition, discrepancies in results could be due to our use of denuded oocytes rather than intact COCs to investigate dose-dependent effects of FF, participant heterogeneity, as well as a lack of knowledge of the maturation status or the fertilization ability of the human gametes from which surrounding FF samples were collected and used for experiments. However, another study that supplemented maturation media with 10%, 30%, and 60% bovine FF demonstrated that 60% FF was associated with decreased development of bovine eggs to the blastocyst stage following fertilization (Kim et al., 1996). Although this endpoint is later in development than those examined in our study,

it provides support that high doses of FF may have negative effects when added to *in vitro* culture systems. Further studies are required to understand what factors within FF may be responsible for these detrimental effects to oocyte quality *in vitro*. Groups that examined the effects of FF on oocyte parameters from different conditions, including different sized follicles and prepubertal versus cycling animals, used 10% FF and saw differences between experimental groups, supporting our use of this concentration to examine age-dependent effects (Pawlak et al., 2018; Park et al., 2021).

Additionally, our observation of robust, dose-dependent effects of FF on meiotic progression may be in part because we utilized denuded oocytes for these experiments. *In vivo*, oocytes are surrounded by cumulus cells, together forming COCs, and cumulus cells are in direct contact with FF within antral follicles. Thus, it is possible that cumulus cells may serve in a protective capacity, which may explain why we observed such detrimental effects of high concentrations of FF.

Given the prominent changes in FF composition with advanced reproductive age, including altered miRNAs and metabolites, imbalance of ROS and antioxidants, as well as increased presence of fibro-inflammatory cytokines, we anticipated observing significant age-associated effects of FF on meiotic progression, spindle assembly, and ploidy (Sang et al., 2013; Battaglia et al., 2020; Bouet et al., 2020; Dogan et al., 2020; Zhang et al., 2020; Machlin et al., 2021). However, other than our finding of reduced meiotic progression of COCs matured in FF from reproductively old participants compared to young counterparts, this was largely not the case and there are a few possible reasons why we did not observe robust age-dependent effects of FF on oocyte nuclear maturation endpoints. In our model system, we performed an acute exposure of oocytes and COCs to FF during the final stages of meiotic maturation for a total of 14–16 h. However, oocytes are surrounded by FF in antral follicles for approximately 80 days during development in humans and ~10 days in mice (Zheng et al., 2014; Williams and Erickson, 2012). Thus, this short-term exposure may not be sufficient for FF components to impact the development and quality of oocytes. However, this cannot easily be addressed experimentally. For example, if we cultured early-stage follicles in media containing FF with the goal of exposing them to FF through development, the follicles would form antrums as they progressed, in turn preventing direct contact between the supplemented FF and oocytes.

Here, we sought to examine the effects of human FF on oocyte quality, and the lack of human oocytes available for research necessitated the use of a heterologous model. In fact, there is precedence for this heterologous model involving supplementation of mouse oocyte maturation media with human FF (Das et al., 1992; Yang et al., 2012). Exposure of mouse oocytes to human FF collected from follicles containing mature eggs competent for fertilization and embryo development has been demonstrated to improve meiotic maturation, including rates of GVBD and PBE, in addition to improving cumulus layer expansion (Das et al., 1992). Moreover, addition of lipid-rich human FF, collected from obese women, to mouse COC maturation media increased oocyte lipid content, induced endoplasmic reticulum stress, and decreased meiotic progression (Yang et al., 2012). However, studies that have investigated the impact of FF on oocyte quality using species-matched FF and oocytes have observed significant reproductive age effects (Takeo et al., 2017). For example, relative to bovine FF from younger animals, samples from older animals resulted in accelerated meiotic progression, elevated ROS content in bovine oocytes, increased rates of abnormal fertilization,

and decreased blastulation rates (Takeo et al., 2017). Thus, it is possible that factors in FF that impact oocyte competence are not conserved between mouse and human.

In this study, we demonstrated that exposure to FF from reproductively old participants significantly increased the size of mitochondrial aggregates compared to exposure to FF from reproductively young counterparts. Although, age-related alterations to mitochondrial morphology, localization, and function have been previously established in the oocyte, our work suggests that some of these alterations may be in part due to exposure to components present in FF from women of advanced reproductive age (Kasapoğlu and Seli, 2020; van der Reest et al., 2021). Mitochondria typically form clusters during nuclear envelope breakdown as well as at telophase I, and this cluster formation is typically associated with increased ATP production (Yu et al., 2010). Large mitochondrial clusters are counterintuitive given that oocytes from old mice have decreased ATP production compared to young counterparts (Kujjo et al., 2013; Ben-Meir et al., 2015; Kim et al., 2020). In fact, we did not observe any differences in ATP production between eggs matured without FF or in media supplemented with FF from reproductively young or old participants. Large aggregates are formed through mitochondrial fusion, which is thought to support ATP production in the presence of cellular stress (Kasapoğlu and Seli, 2020). Thus, the mitochondrial aggregation we observed following maturation in media containing FF from reproductively old participants may be a compensatory mechanism to increase ATP production. Although we did not observe an immediate effect of larger mitochondrial aggregates on ATP production, it is possible that the effects may manifest later during embryo development. Further studies are warranted to determine whether FF exposure during maturation affects fertilization and early embryo development in an age-dependent manner. However, such experiments pose a technical challenge as oocytes matured *in vitro* may undergo hardening of the zona pellucida, in turn necessitating the use of intracytoplasmic sperm injection, rather than conventional *in vitro* fertilization (De Vos and Van Steirteghem, 2000; Kilani et al., 2006). Mitochondria also aggregate in response to apoptotic stimuli, resulting in cytochrome c release, and ultimately caspase activation (Haga et al., 2003). It is therefore possible that larger mitochondrial aggregates in oocytes exposed to FF from reproductively old participants is indicative of the early stages of apoptosis. Moreover, we observed a greater tendency of eggs matured in FF from reproductively old participants to display a clustering distribution compared to eggs matured without FF or in FF from reproductively young participants, although this phenotype was not significant. This is interesting as mitochondria in oocytes from aged mice have been shown to form clusters in the ooplasm, rather than displaying an association with the meiotic spindle and chromosomes (Kim et al., 2020). Thus, the aging FF microenvironment may contribute to impaired mitochondrial distribution with age.

We demonstrated that FF had an age-dependent impact on cumulus expansion kinetics in COCs from reproductively old mice. As cumulus layer expansion is important for ovulation and fertilization, it is possible that the altered expansion kinetics we observed upon treatment with FF from reproductively old participants may impact these processes. In fact, ovulation is impaired with advanced age and reproductively old mice ovulate fewer eggs, have fewer corpora lutea (CLs), and have more frequent failed ovulations, as indicated by trapped oocytes in CLs and expanded COCs in unruptured follicles, compared to reproductively young counterparts (Mara et al., 2020). Future studies are needed

to investigate the role of FF in these phenotypes. Moreover, it is possible that FF has age-dependent effects on cumulus cells at a molecular level. Studies that have treated fallopian tube epithelial (FTE) cells with FF to study ovarian cancer initiation determined that FF exposure increases DNA damage in FTE cells and it is possible that FF has similar effects on cumulus cells (Brachova et al., 2017).

Here, we sought to understand the impact of human FF on the oocyte and to this end, we developed a heterologous assay that allowed us to overcome the barrier for research with human tissue. We examined the dose- and age-dependent effects of human FF on mouse oocyte competence. We demonstrated that the oocyte is responsive to the FF environment, however, for the most part, not in an age-dependent manner. Although we cannot rule out the fact that we did not observe robust age-associated phenotypes due to the differences in species and the acute exposure of oocytes to FF in our model, it is also possible that oocyte-intrinsic mechanisms are the primary factors leading to the age-related decline in gamete quality.

## Supplementary data

Supplementary data are available at *Molecular Human Reproduction* online.

## Data availability

All original data in this publication are available upon reasonable request to the corresponding author.

## Acknowledgements

We thank all members of the Duncan lab for their support and valuable discussion regarding this work. We thank Rafael Confino, Shriya Shah, and Asma Giomazi for assistance with follicular fluid acquisition, as well as Maxwell Shramuk at the Biostatistics Collaboration Center and Dr. Elnur Babayev for their expertise on statistical analysis. ATP measurement was performed using equipment from the Analytical bioNanoTechnology Core Facility (ANTEC) of the Simpson Querrey Institute for BioNanotechnology at Northwestern University. ANTEC is currently supported by the Soft and Hybrid Nanotechnology Experimental (SHyNE) Resource (NSF ECCS-2025633).

## Authors' roles

S.S.D. and F.E.D. designed the experiments. S.S.D. and C.S. performed the experiments and analyzed the data. All authors provided critical feedback and contributed to interpretation of results. S.S.D. prepared the original draft of the manuscript and all authors reviewed and edited the manuscript. All authors have read and agreed to the published version of the manuscript.

## Funding

This work was supported by startup funds from the Department of Obstetrics and Gynecology, Feinberg School of Medicine, Northwestern University (to F.E.D.), the Eunice Kennedy Shriver National Institute of Child Health and Human Development (T32HD094699 to S.S.D.), and the National Cancer Institute (F31CA257300 to S.S.D. and CA240301 and CA240423 to J.E.B.).

## Conflict of interest

The authors declare no conflicts of interest.

## References

- Azari-Dolatabad N, Raes A, Pavani KC, Asaadi A, Angel-Velez D, Van Damme P, Leroy JLMR, Van Soom A, Pascottini OB. Follicular fluid during individual oocyte maturation enhances cumulus expansion and improves embryo development and quality in a dose-specific manner. *Theriogenology* 2021;**166**:38–45.
- Babayev E, Duncan FE. Age-associated changes in cumulus cells and follicular fluid: the local oocyte microenvironment as a determinant of gamete quality. *Biol Reprod* 2022;**106**:351–365.
- Babayev E, Seli E. Oocyte mitochondrial function and reproduction. *Curr Opin Obstet Gynecol* 2015;**27**:175–181.
- Battaglia R, Musumeci P, Ragusa M, Barbagallo D, Scalia M, Zimbone M, Lo Faro JM, Borzì P, Scollo P, Purrello M et al. Ovarian aging increases small extracellular vesicle CD81(+) release in human follicular fluid and influences miRNA profiles. *Aging (Albany NY)* 2020;**12**:12324–12341.
- Bebere D, Cotichio G, Borini A, Ledda S. Oocyte aging: looking beyond chromosome segregation errors. *J Assist Reprod Genet* 2022;**39**:793–800.
- Ben-Meir A, Burstein E, Borrego-Alvarez A, Chong J, Wong E, Yavorska T, Naranian T, Chi M, Wang Y, Bentov Y et al. Coenzyme Q10 restores oocyte mitochondrial function and fertility during reproductive aging. *Aging Cell* 2015;**14**:887–895.
- Bouet P-E, Boueilh T, de la Barca JMC, Boucrot L, Blanchard S, Ferré L'Hotellier V, Jeannin P, Descamps P, Procaccio V, Reynier P. The cytokine profile of follicular fluid changes during ovarian ageing. *J Gynecol Obstet Hum Reprod* 2020;**49**:101704.
- Brachova P, Alvarez NS, Van Voorhis BJ, Christenson LK. Cytidine deaminase Apobec3a induction in fallopian epithelium after exposure to follicular fluid. *Gynecol Oncol* 2017;**145**:577–583.
- Cheng JM, Li J, Tang JX, Hao XX, Wang ZP, Sun TC, Wang XX, Zhang Y, Chen SR, Liu YX. Merotelic kinetochore attachment in oocyte meiosis II causes sister chromatids segregation errors in aged mice. *Cell Cycle* 2017;**16**:1404–1413.
- Chiang T, Duncan FE, Schindler K, Schultz RM, Lampson MA. Evidence that weakened centromere cohesion is a leading cause of age-related aneuploidy in oocytes. *Curr Biol* 2010;**20**:1522–1528.
- Clarke H. Control of mammalian oocyte development by interactions with the maternal follicular environment. *Results Probl Cell Differ* 2017;**63**:17–41.
- Clarke HJ. Transzonal projections: essential structures mediating intercellular communication in the mammalian ovarian follicle. *Mol Reprod Dev* 2022;**89**:509–525.
- Conti M, Franciosi F. Acquisition of oocyte competence to develop as an embryo: integrated nuclear and cytoplasmic events. *Hum Reprod Update* 2018;**24**:245–266.
- Cordeiro FB, Montani DA, Pilau EJ, Gozzo FC, Fraietta R, Turco EGL. Ovarian environment aging: follicular fluid lipidomic and related metabolic pathways. *J Assist Reprod Genet* 2018;**35**:1385–1393.
- D'Aniello G, Grieco N, Di Filippo MA, Cappiello F, Topo E, D'Aniello E, Ronsini S. Reproductive implication of D-aspartic acid in human pre-ovulatory follicular fluid. *Hum Reprod* 2007;**22**:3178–3183.
- Dalton CM, Carroll J. Biased inheritance of mitochondria during asymmetric cell division in the mouse oocyte. *J Cell Sci* 2013;**126**:2955–2964.
- Das K, Phipps WR, Hensleigh HC, Tagatz GE. Epidermal growth factor in human follicular fluid stimulates mouse oocyte maturation in vitro. *Fertil Steril* 1992;**57**:895–901.

- De Vos A, Van Steirteghem A. Zona hardening, zona drilling and assisted hatching: new achievements in assisted reproduction. *Cells Tissues Organs* 2000;**166**:220–227.
- Dell'Aquila ME, Cho YS, Minoia P, Traina V, Lacalandra GM, Maritato F. Effects of follicular fluid supplementation of in-vitro maturation medium on the fertilization and development of equine oocytes after in-vitro fertilization or intracytoplasmic sperm injection. *Hum Reprod* 1997;**12**:2766–2772.
- Dogan B, Karaer A, Tuncay G, Tecellioglu N, Mumcu A. High-resolution (1)H-NMR spectroscopy indicates variations in metabolomics profile of follicular fluid from women with advanced maternal age. *J Assist Reprod Genet* 2020;**37**:321–330.
- Doherty CA, Amargant F, Shvartsman SY, Duncan FE, Gavis ER. Bidirectional communication in oogenesis: a dynamic conversation in mice and Drosophila. *Trends Cell Biol* 2022;**32**:311–323.
- Dumesic DA, Meldrum DR, Katz-Jaffe MG, Krisher RL, Schoolcraft WB. Oocyte environment: follicular fluid and cumulus cells are critical for oocyte health. *Fertil Steril* 2015;**103**:303–316.
- Duncan FE, Chiang T, Schultz RM, Lampson MA. Evidence that a defective spindle assembly checkpoint is not the primary cause of maternal age-associated aneuploidy in mouse eggs. *Biol Reprod* 2009;**81**:768–776.
- Edwards RG. Follicular fluid. *J Reprod Fertil* 1974;**37**:189–219.
- Emori MM, Drapkin R. The hormonal composition of follicular fluid and its implications for ovarian cancer pathogenesis. *Reprod Biol Endocrinol* 2014;**12**:60.
- Haga N, Fujita N, Tsuruo T. Mitochondrial aggregation precedes cytochrome c release from mitochondria during apoptosis. *Oncogene* 2003;**22**:5579–5585.
- Hassold T, Hunt P. To err (meiotically) is human: the genesis of human aneuploidy. *Nat Rev Genet* 2001;**2**:280–291.
- Hayashi K, Hikabe O, Obata Y, Hirao Y. Reconstitution of mouse oogenesis in a dish from pluripotent stem cells. *Nat Protoc* 2017;**12**:1733–1744.
- Hennet ML, Combelles CM. The antral follicle: a microenvironment for oocyte differentiation. *Int J Dev Biol* 2012;**56**:819–831.
- Kang H-G, Cha B-H, Jun J-H. Alteration of spindle formation and chromosome alignment in post-ovulatory aging of mouse oocytes. *Dev Reprod* 2011;**15**:231–237.
- Kasapoğlu I, Seli E. Mitochondrial dysfunction and ovarian aging. *Endocrinology* 2020;**161**:bqaa001.
- Kilani SS, Cooke S, Kan AK, Chapman MG. Do age and extended culture affect the architecture of the zona pellucida of human oocytes and embryos? *Zygote* 2006;**14**:39–44.
- Kim K, Mitsumizo N, Fujita K, Utsumi K. The effects of follicular fluid on in vitro maturation, oocyte fertilization and the development of bovine embryos. *Theriogenology* 1996;**45**:787–799.
- Kim MJ, Choi KH, Seo DW, Lee HR, Kong HS, Lee CH, Lee WS, Lee HT, Ko JJ, Kim JH et al. Association between functional activity of mitochondria and actin cytoskeleton instability in oocytes from advanced age mice. *Reprod Sci* 2020;**27**:1037–1046.
- Krisher RL. Maternal age affects oocyte developmental potential at both ends of the age spectrum. *Reprod Fertil Dev* 2018;**31**:1–9.
- Kujjo LL, Acton BM, Perkins GA, Ellisman MH, D'Estaing SG, Casper RF, Jurisicova A, Perez GI. Ceramide and its transport protein (CERT) contribute to deterioration of mitochondrial structure and function in aging oocytes. *Mech Ageing Dev* 2013;**134**:43–52.
- Kusuhara A, Babayev E, Zhou LT, Singh VP, Gerton JL, Duncan FE. Immature follicular origins and disrupted oocyte growth pathways contribute to decreased gamete quality during reproductive juvenescence in mice. *Front Cell Dev Biol* 2021;**9**:693742.
- Liu L, Keefe DL. Defective cohesin is associated with age-dependent misaligned chromosomes in oocytes. *Reprod Biomed Online* 2008;**16**:103–112.
- Machlin JH, Barishansky SJ, Kelsh J, Larmore MJ, Johnson BW, Pritchard MT, Pavone ME, Duncan FE. Fibroinflammatory signatures increase with age in the human ovary and follicular fluid. *Int J Mol Sci* 2021;**22**:4902.
- Mara JN, Zhou LT, Larmore M, Johnson B, Ayiku R, Amargant F, Pritchard MT, Duncan FE. Ovulation and ovarian wound healing are impaired with advanced reproductive age. *Aging (Albany NY)* 2020;**12**:9686–9713.
- Mikwar M, MacFarlane AJ, Marchetti F. Mechanisms of oocyte aneuploidy associated with advanced maternal age. *Mutat Res Rev Mutat Res* 2020;**785**:108320.
- Nagyova E. The biological role of hyaluronan-rich oocyte-cumulus extracellular matrix in female reproduction. *Int J Mol Sci* 2018;**19**:283.
- Oyawoye O, Abdel Gadir A, Garner A, Constantinovici N, Perrett C, Hardiman P. Antioxidants and reactive oxygen species in follicular fluid of women undergoing IVF: relationship to outcome. *Hum Reprod* 2003;**18**:2270–2274.
- Park J-E, Lee S-H, Hwangbo Y, Park C-K. Porcine follicular fluid derived from >8 mm sized follicles improves oocyte maturation and embryo development during in vitro maturation of pigs. *Zygote* 2021;**29**:27–32.
- Pasqualotto EB, Agarwal A, Sharma RK, Izzo VM, Pinotti JA, Joshi NJ, Rose BI. Effect of oxidative stress in follicular fluid on the outcome of assisted reproductive procedures. *Fertil Steril* 2004;**81**:973–976.
- Pawlak P, Warzych E, Cieslak A, Malyszka N, Maciejewska E, Madeja ZE, Lechniak D. The consequences of porcine IVM medium supplementation with follicular fluid become reflected in embryo quality, yield and gene expression patterns. *Sci Rep* 2018;**8**:15306.
- Piperi C, Adamopoulos C, Dalagiorgou G, Diamanti-Kandaraki E, Papavassiliou AG. Crosstalk between advanced glycation and endoplasmic reticulum stress: emerging therapeutic targeting for metabolic diseases. *J Clin Endocrinol Metab* 2012;**97**:2231–2242.
- Revelli A, Delle Piane L, Casano S, Molinari E, Massobrio M, Rinaudo P. Follicular fluid content and oocyte quality: from single biochemical markers to metabolomics. *Reprod Biol Endocrinol* 2009;**7**:40.
- Robker RL, Hennebold JD, Russell DL. Coordination of ovulation and oocyte maturation: a good egg at the right time. *Endocrinology* 2018;**159**:3209–3218.
- Rodgers RJ, Irving-Rodgers HF. Formation of the ovarian follicular antrum and follicular fluid. *Biol Reprod* 2010;**82**:1021–1029.
- Rogers HB, Zhou LT, Kusuhara A, Zaniker E, Shafae S, Owen BC, Duncan FE, Woodruff TK. Dental resins used in 3D printing technologies release ovo-toxic leachates. *Chemosphere* 2021;**270**:129003.
- Ruebel ML, Piccolo BD, Mercer KE, Pack L, Moutos D, Shankar K, Andres A. Obesity leads to distinct metabolomic signatures in follicular fluid of women undergoing in vitro fertilization. *Am J Physiol Endocrinol Metab* 2019;**316**:E383–E396.
- Sang Q, Yao Z, Wang H, Feng R, Wang H, Zhao X, Xing Q, Jin L, He L, Wu L et al. Identification of microRNAs in human follicular fluid: characterization of microRNAs that govern steroidogenesis in vitro and are associated with polycystic ovary syndrome in vivo. *J Clin Endocrinol Metab* 2013;**98**:3068–3079.
- Schon SB, Yang K, Schindler R, Jiang L, Neff LM, Seeley RJ, Marsh EE. Obesity-related alterations in protein expression in human follicular fluid from women undergoing in vitro fertilization. *F S Sci* 2022;**3**:331–339.
- Somfai T, Inaba Y, Watanabe S, Geshi M, Nagai T. Follicular fluid supplementation during in vitro maturation promotes sperm penetration in bovine oocytes by enhancing cumulus expansion

- and increasing mitochondrial activity in oocytes. *Reprod Fertil Dev* 2012;**24**:743–752.
- Song J, Xiang S, Pang C, Guo J, Sun Z. Metabolomic alternations of follicular fluid of obese women undergoing in-vitro fertilization treatment. *Sci Rep* 2020;**10**:5968.
- Suebthawinkul C, Babayev E, Lee HC, Duncan FE. Morphokinetic parameters of mouse oocyte meiotic maturation and cumulus expansion are not affected by reproductive age or ploidy status. *J Assist Reprod Genet* 2023;**40**:1197–1213.
- Suebthawinkul C, Babayev E, Zhou LT, Lee HC, Duncan FE. Quantitative morphokinetic parameters identify novel dynamics of oocyte meiotic maturation and cumulus expansion†. *Biol Reprod* 2022;**107**:1097–1112.
- Takeo S, Kimura K, Shirasuna K, Kuwayama T, Iwata H. Age-associated deterioration in follicular fluid induces a decline in bovine oocyte quality. *Reprod Fertil Dev* 2017;**29**:759–767.
- Tian H, Liu K, Zhang Y, Qi Q, Wang C, Guan H, Yan F, Hou J. Adult follicular fluid supplementation during in vitro maturation improves the developmental competence of prepubertal lamb oocytes. *Theriogenology* 2019;**130**:157–162.
- Tomari H, Honjo K, Kunitake K, Aramaki N, Kuhara S, Hidaka N, Nishimura K, Nagata Y, Horiuchi T. Meiotic spindle size is a strong indicator of human oocyte quality. *Reprod Med Biol* 2018;**17**:268–274.
- Van Blerkom J, Antczak M, Schrader R. The developmental potential of the human oocyte is related to the dissolved oxygen content of follicular fluid: association with vascular endothelial growth factor levels and perifollicular blood flow characteristics. *Hum Reprod* 1997;**12**:1047–1055.
- van der Reest J, Nardini Cecchino G, Haigis MC, Kordowitzki P. Mitochondria: their relevance during oocyte ageing. *Ageing Res Rev* 2021;**70**:101378.
- Verlhac M-H, Terret M-E. *Mouse Oocyte Development: Methods and Protocols*. New York, NY, USA: Springer, 2018.
- Wakai T, Harada Y, Miyado K, Kono T. Mitochondrial dynamics controlled by mitofusins define organelle positioning and movement during mouse oocyte maturation. *Mol Hum Reprod* 2014;**20**:1090–1100.
- Wang Q, Ratchford AM, Chi MM, Schoeller E, Frolova A, Schedl T, Moley KH. Maternal diabetes causes mitochondrial dysfunction and meiotic defects in murine oocytes. *Mol Endocrinol* 2009;**23**:1603–1612.
- Wang S, Zheng Y, Li J, Yu Y, Zhang W, Song M, Liu Z, Min Z, Hu H, Jing Y et al. Single-cell transcriptomic atlas of primate ovarian aging. *Cell* 2020;**180**:585–600.e19.
- Williams CJ, Erickson GF. *Morphology and Physiology of the Ovary*. In: Feingold KR, Anawalt B, Blackman MR, Boyce A, Chrousos G, Corpas E, de Herder WW, Dhatariya K, Dungan K, Hofland J et al. (eds). *Endotext* [Internet]. South Dartmouth, MA, USA: MDText.com, Inc., 2012. <https://www.ncbi.nlm.nih.gov/books/NBK278951/>
- Yamada M, Isaji Y. Structural and functional changes linked to, and factors promoting, cytoplasmic maturation in mammalian oocytes. *Reprod Med Biol* 2011;**10**:69–79.
- Yang L, Baumann C, De La Fuente R, Viveiros MM. Mechanisms underlying disruption of oocyte spindle stability by bisphenol compounds. *Reproduction* 2020;**159**:383–396.
- Yang X, Wu LL, Chura LR, Liang X, Lane M, Norman RJ, Robker RL. Exposure to lipid-rich follicular fluid is associated with endoplasmic reticulum stress and impaired oocyte maturation in cumulus-oocyte complexes. *Fertil Steril* 2012;**97**:1438–1443.
- Yu Y, Dumollard R, Rossbach A, Lai FA, Swann K. Redistribution of mitochondria leads to bursts of ATP production during spontaneous mouse oocyte maturation. *J Cell Physiol* 2010;**224**:672–680.
- Zeng J, Jiang M, Wu X, Diao F, Qiu D, Hou X, Wang H, Li L, Li C, Ge J et al. SIRT4 is essential for metabolic control and meiotic structure during mouse oocyte maturation. *Ageing Cell* 2018;**17**:e12789.
- Zhang M, Lu Y, Chen Y, Zhang Y, Xiong B. Insufficiency of melatonin in follicular fluid is a reversible cause for advanced maternal age-related aneuploidy in oocytes. *Redox Biol* 2020;**28**:101327.
- Zheng W, Zhang H, Liu K. The two classes of primordial follicles in the mouse ovary: their development, physiological functions and implications for future research. *Mol Hum Reprod* 2014;**20**:286–292.